Knockout of juvenile hormone receptor, Methoprene-tolerant, induces black larval phenotype in the yellow fever mosquito, *Aedes aegypti*

Guan-Heng Zhu[a], Yaoyu Jiao[a], Shankar C. R. R. Chereddy[a], Mi Young Noh[b], and Subba Reddy Palli[a,1]

[a]Department of Entomology, College of Agriculture, Food and Environment, University of Kentucky, Lexington, KY 40546; and [b]Department of Forestry, Chonnam National University, Gwangju, 61186 South Korea

Edited by Lynn M. Riddiford, University of Washington, Friday Harbor, WA, and approved September 13, 2019 (received for review April 3, 2019)

The yellow fever mosquito, *Aedes aegypti*, vectors human pathogens. Juvenile hormones (JH) control almost every aspect of an insect's life, and JH analogs are currently used to control mosquito larvae. Since RNA interference does not work efficiently during the larval stages of this insect, JH regulation of larval development and mode of action of JH analogs are not well studied. To overcome this limitation, we used a multiple single guide RNA-based CRISPR/Cas9 genome-editing method to knockout the *methoprene-tolerant* (*Met*) gene coding for a JH receptor. The *Met* knockout larvae exhibited a black larval phenotype during the L3 (third instar larvae) and L4 (fourth instar larvae) stages and died before pupation. However, *Met* knockout did not affect embryonic development or the L1 and L2 stages. Microscopy studies revealed the precocious synthesis of a dark pupal cuticle during the L3 and L4 stages. Gene expression analysis showed that *Krüppel homolog 1*, a key transcription factor in JH action, was down-regulated, but genes coding for proteins involved in melanization, pupal and adult cuticle synthesis, and blood meal digestion in adults were up-regulated in L4 *Met* mutants. These data suggest that, during the L3 and L4 stages, *Met* mediates JH suppression of pupal/adult genes involved in the synthesis and melanization of the cuticle and blood meal digestion. These results help to advance our knowledge of JH regulation of larval development and the mode of action of JH analogs in *Ae. aegypti*.

CRISPR/Cas9 | gene editing | sgRNA | cuticle | metamorphosis

Juvenile hormones (JH) and ecdysteroids [20-hydroxyecdysone (20E) is the most active form] regulate molting and metamorphosis in insects (1, 2). While 20E initiates a cascade of gene expression and repression events during molting, JH preserves the juvenile status preventing metamorphosis (1, 2). Thus, during the larval stages, JH suppresses the expression of pupal and adult genes to ensure that the next molt is into a larva rather than metamorphosis to pupa or adult. At the end of the larval stage, JH levels decrease, allowing 20E to induce expression of pupal/adult genes resulting in metamorphosis to pupa or adult (1, 2). The *methoprene-tolerant* (*Met*) gene was discovered in the fruit fly, *Drosophila melanogaster*, based on the mutations that confer resistance to the JH analog, methoprene (3). However, Met was not confirmed as a JH receptor due to the lack of distinct effects of the *Met* mutation on *D. melanogaster* development. Studies in the red flour beetle, *Tribolium castaneum*, where RNA interference (RNAi)-mediated knockdown of *Met* induces precocious metamorphosis and premature development of pupal and adult structures, confirmed Met as a JH receptor (4). Later, it was shown that the *D. melanogaster* genome codes for 2 genes, *Met* and its paralog, *germ cell-expressed* (*gce*); mutation of *Met* and deletion of *gce* simultaneously induced lethality during metamorphosis similar to the mortality detected in allatectomized pupae (5). The Met protein binds to JH with a high affinity (6). In *D. melanogaster*, expression of *Met*/*gce* can rescue flies with *Met* mutations and *gce* deletion, establishing Met/gce as a JH receptor (7). Studies in multiple insects established Met, a member of the basic helix-loop-helix–Per-Arnt-Sim transcription factor family, as a JH receptor (2). Met functions through the recruitment of Taiman and induces the expression of JH-response genes, including the gene coding for a transcription factor, Krüppel homolog 1 (Kr-h1) (8, 9). During immature stages, Kr-h1 suppresses the expression of genes coding for the pupal specifier, Broad-Complex (BR-C) (10) and the adult specifier, E93 (11).

Overexpression of a gene coding for a JH-degrading enzyme, *JH esterase* (*jhe*), in *Bombyx mori* induced precocious metamorphosis from the third instar larval stage (12). Also, JH deficiency due to the null mutation of *dimolting* in *B. mori* induced metamorphosis in miniature pupae after the L3 or L4 stage (13). Furthermore, blocking the JH response by knocking out a gene coding for a JH biosynthesis enzyme, JH acid methyltransferase (jhamt), or Met induced precocious development of pupal structures in the L4 stage (14). These experiments showed that *B. mori* embryogenesis and early larval development do not require Met.

The yellow fever mosquito *Aedes aegypti* transmits many arboviruses that cause diseases such as yellow fever, dengue fever, Zika fever, and chikungunya. The JH analog, methoprene, is widely used for controlling *Ae. aegypti* and other mosquito larvae. The function of Met in JH regulation of *Ae. aegypti* female reproduction has been well studied (15). RNAi-mediated knockdown of *Cycle* (*CYC*) and *Met* showed that the Met/CYC heterodimer

Significance

Juvenile hormone (JH) analogs are used to control mosquitoes. However, both larval development and action of JH analogs are not well studied in these insects because RNA interference does not work well. A multiple single guide RNA-based CRISPR/Cas9 genome-editing method was used to knockout the *methoprene-tolerant* gene (*Met*, a JH receptor). The *Met* knockout larvae showed precocious development of pupal cuticle and expression of pupal/adult genes involved in the synthesis and melanization of cuticle and blood meal digestion. The methods developed here could help to overcome the major hurdle in functional genomics studies in *Aedes aegypti* and facilitate advances in understanding larval development and mode of action of JH analogs.

Author contributions: G.-H.Z. and S.R.P. designed research; G.-H.Z., Y.J., S.C.R.R.C., and M.Y.N. performed research; G.-H.Z., Y.J., S.C.R.R.C., M.Y.N., and S.R.P. analyzed data; and G.-H.Z. and S.R.P. wrote the paper.

The authors declare no competing interest.

This article is a PNAS Direct Submission.

Data deposition: The short read (BGISEQ-500) data reported in this paper have been deposited in the National Center for Biotechnology Information BioProject database, https://www.ncbi.nlm.nih.gov/bioproject?term=PRJNA551480 (accession no. PRJNA551480).

[1]To whom correspondence may be addressed. Email: rpalli@uky.edu.

This article contains supporting information online at www.pnas.org/lookup/suppl/doi:10.1073/pnas.1905729116/-/DCSupplemental.

First published September 30, 2019.

mediates JH activation of *Kr-h1* and *Hairy* genes in female mosquitoes (16). However, JH action during larval stages and mode of action of JH analogs are not well studied because it is challenging to manipulate *Ae. aegypti* larvae that are growing in water and also due to problems associated with the delivery of double-stranded RNA and its stability; RNAi is inefficient in larval stages when compared to other stages of this insect.

Various genome-editing methods, including CRISPR/Cas9, have been used to knock out genes in *Ae. aegypti* (17–23). To improve the chances of identification of CRISPR/Cas9-induced gene knockouts in *Ae. aegypti*, we injected multiple single guide RNAs (sgRNAs) targeting the gene coding for Met into embryos and detected a loss-of-function phenotype in G0. The *Met* knockout larvae exhibited a black larval phenotype during L3 and L4 and died during the late larval stage before pupation. Gene expression studies revealed that during larval stages Met suppresses pupal and adult genes, including those coding for proteins involved in pupal/adult cuticle synthesis, melanization, and blood meal digestion.

Results and Discussion

Multiple sgRNAs Improve Detection of the Loss-of-Function Phenotype in G0. Previous studies in *Ae. aegypti* reported CRISPR/Cas9-induced mutations of the gene coding for the enzyme kynurenine 3-monooxygenase (kmo), which is involved in eye pigmentation (17, 20). Methods for CRISPR/Cas9-mediated genome editing in *Ae. aegypti* were developed by multiple groups (17, 18, 24) and used to study sex determination (19), microRNA function (21, 23), and insulin signaling (22). In most cases, mutant phenotypes have been detected in the offspring developed from CRISPR/Cas9-injected embryos. However, in some cases, identification of a loss-of-function phenotype for studying the function of a target gene may require establishing a homozygous line. In the preliminary studies, injection of 1 sgRNA targeting the *kmo* gene into *Ae. aegypti* embryos showed a mosaic-eye phenotype in G0. We tested the injection of multiple sgRNAs to determine if the detection rate of the loss-of-function phenotype in G0 could be improved. Four sgRNAs were designed targeting exon 5 and introns on either side of this exon of the *kmo* gene (*SI Appendix*, Fig. S1*A*). Injection of 1 sgRNA/Cas9 (sgRNA-B) targeting exon 5 induced a mosaic-eye phenotype in 40% (36/90) of larvae and the pupae developed from injected eggs (*SI Appendix*, Table S1). Only 1 larva displayed the complete white-eye phenotype in G0, which is similar to the white-eye phenotype observed in the compound heterozygous G1 insects obtained after injection of sgRNA/Cas9 and self-crossing (*SI Appendix*, Fig. S1*B*). Injection of 2 sgRNAs (one targeting exon 5, sgRNA-B and the other targeting the intron, sgRNA-A) induced mosaic eyes in 50% (40/80) of larvae and pupae (*SI Appendix*, Table S1), but a complete white-eye phenotype was not detected in any of the G0 larvae. In contrast, injection of 3 sgRNAs targeting exon 5 and an intron (sgRNA-A, sgRNA-B, and sgRNA-C) induced a white-eye phenotype in 11% (21/190) of G0 larvae and pupae (*SI Appendix*, Table S1). Also, the injection of 4 sgRNAs (sgRNA-A, sgRNA-B, sgRNA-C, and sgRNA-D) induced a white-eye phenotype in 19–23% (32/165, 42/180) of G0 larvae and pupae (*SI Appendix*, Table S1). These data suggest that multiple sgRNAs could induce a high frequency of fragment deletions between different target sites, resulting in an increase in detection of loss of function in G0 (*SI Appendix*, Fig. S1*B*). To analyze the mutation frequency in white-eye phenotype insects, 12 white-eye pupae were randomly selected for isolation of genomic DNA and PCR amplification of the target gene. The mutation rate was quantified by the T7 Endonuclease I (T7E1) assay. As shown in *SI Appendix*, Fig. S2*A*, the PCR products revealed multiple bands suggesting that a high frequency of long fragment deletions was induced in the target gene. Compared to wild type (WT), the mutant DNA showed low-intensity WT gene fragments. The mutation efficiency of each line was quantified based on the band intensity in the gel. The average mutation efficiency was estimated to be 94% (*SI Appendix*, Fig. S2*B*). Because T7E1 recognizes and cleaves imperfectly matched DNA, if the 2 strands of hybridized PCR products had the same mutation, the T7E1 could not cleave the fragment at the mutation site. Therefore, the 94% mutation rate calculated could be an underestimate. The PCR products were sequenced, and the sequencing data showed mutations in DNA isolated from all mutants; some of the mutants showed the same deletions (*SI Appendix*, Fig. S3). Taken together, the T7E1 and sequencing data suggest that injection of multiple sgRNAs induced a loss-of-function phenotype of the *kmo* gene, inducing the white-eye phenotype in the G0 generation.

Recently, Li et al. (20) produced transgenic *Ae. aegypti* expressing the *Cas9* gene under the control of the AAEL010097 promoter (AAEL010097-Cas9 strain). Injection of sgRNA into eggs of this strain showed an improvement in sgRNA-induced mutagenesis when compared to injection of sgRNA/Cas9 into WT strain eggs. We tested *kmo* sgRNA combinations in the AAEL010097-Cas9 strain. Injection of each single sgRNA-A, sgRNA-B, sgRNA-C, and sgRNA-D induced a mosaic-eye phenotype in 0, 70 (67/97), 48 (31/65), and 0% of larvae and the white-eye phenotype in 0, 8 (8/97), 6 (4/65), and 0% of larvae, respectively (*SI Appendix*, Table S1). While injection of 2, 3, or 4 sgRNAs induced a mosaic-eye phenotype in 46% (77/166), 59% (109/183), and 81% (104/127) and the white-eye phenotype in 4% (7/166), 25% (46/183), and 50% (65/127) of insects, respectively (*SI Appendix*, Fig. S4*A* and Table S1). Mutations in the target gene in white-eye insects were confirmed by sequencing (*SI Appendix*, Fig. S4 *B* and *C*). In each sgRNA combination tested, the loss-of-function phenotype frequency of the AAEL010097-Cas9 strain was higher than that observed in the Liverpool IB12 strain (*SI Appendix*, Table S1). These data demonstrate that the use of the AAEL010097-Cas9 strain could increase sgRNA/Cas9-induced mutation efficiency.

Detection of a Loss-of-Function Phenotype of the *Met* Gene in G0. To achieve a loss-of-function phenotype of the *Met* gene in G0, 4 sgRNAs were designed targeting exons 2 and 4 of the *Met* gene (Fig. 1*A*). The 4 sgRNAs were injected into AAEL010097-Cas9 strain eggs and 22 to 31% of the injected eggs hatched (*SI Appendix*, Table S2). Interestingly, 25 to 48% of the hatched larvae exhibited a black larval phenotype (Fig. 1*B* and *SI Appendix*, Table S2) beginning in L3, and these larvae started dying during the L4 stage before entering the pupal stage. The black color of the skin was lighter and showed a mosaic pattern during L3 but was uniformly dark during L4. We also found that the abdomen of the *Met* loss-of-function phenotype 48-h-old L4 larvae is similar to that of the 24-h-old pupa (dark and shorter); the WT 48-h-old L4 larva did not show any dark pupal abdomen phenotype (Fig. 1*B*). The mutations in the *Met* gene in the black larvae were confirmed by sequencing (Fig. 1*C*). To test the mutation efficiency of each sgRNA, 4 sgRNAs were injected individually into eggs. Only larvae derived from *Met*-sgRNA-C and *Met*-sgRNA-D–injected eggs showed 14 and 9% black larval phenotype, respectively (Fig. 1*D* and *SI Appendix*, Table S2). The injection of 2 sgRNAs (*Met*-sgRNA-C and *Met*-sgRNA-D) induced 25% black larval phenotypes in G0 L3 and L4 (Fig. 1*D* and *SI Appendix*, Table S2). Mutations in each *Met* sgRNA target site were confirmed by sequencing (*SI Appendix*, Fig. S5). These data on *Met* mutations confirm data obtained with marker gene mutations and demonstrate that a multiple sgRNA-based method could be used to improve chances of identifying gene knockout phenotypes in G0. Recent studies in *D. melanogaster* reported improvement in the frequency of CRISPR/Cas9 editing of genes when 2 or more sgRNAs are used (25–27).

The off-target effects caused by single or multiple sgRNAs are a concern that needs to be addressed in gene-editing experiments (28). The sgRNAs were designed and evaluated for their potential off-target effects using the CRISPR optimal

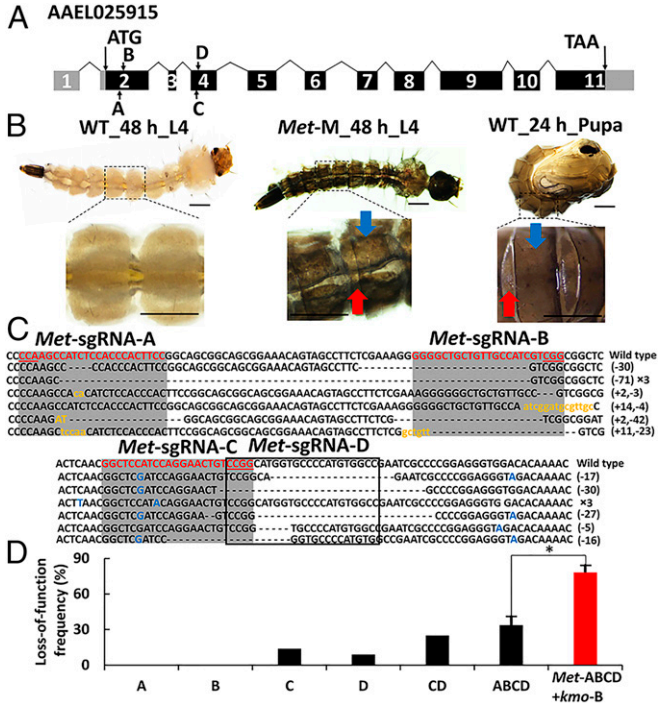

Fig. 1. Knockout of the *Met* gene by CRISPR/Cas9-mediated genome editing using multiple sgRNAs. (*A*) Schematic diagram of the AAEL025915 (*Met*) gene and sgRNA design. (*B*) Mutant phenotype of *Met* gene during the fourth instar larval stage. Pictures of abdominal segments of 48-h-old WT L4, 48-h-old *Met* knockout L4, and 24-h-old WT pupa are shown. The articulations are indicated by blue arrows, and the lateral plates are indicated by red arrows. *Met*-M, *Met* mutant. (Scale bar, 1 mm.) (*C*) Sequences of *Met* gene from WT and mutants determined by TA cloning and sequencing. The WT sequence is shown at the top with the sgRNA target sites in red letters, and protospacer adjacent motif (PAM) sequences underlined. The sgRNA-A, sgRNA-B, and sgRNA-C are shadowed in gray, and sgRNA-D is indicated by a rectangle. In the mutant sequences, deletions are shown as dashes and insertions as yellow lowercase letters. The base transitions are shown in blue letters. The net change in length is shown at the right of each sequence (–, deletion; +, insertion). The number of times that each mutant sequence isolated is shown by a multiplication sign. (*D*) Comparison of the knockout frequencies of the *Met* gene in larvae developed from eggs injected with single or multiple *Met* sgRNAs or single *kmo* sgRNA plus multiple *Met* sgRNAs. The mutant larvae developed from *Met* and *kmo* sgRNA-injected eggs were selected in L2 based on eye phenotype. The data for *Met*-sgRNA-ABCD and *Met*-sgRNA-ABCD + *kmo*-sgRNA-B shown are mean + SE ($n = 3$). The asterisk indicates the significant differences between the 2 groups (*$P < 0.05$). A, *Met*-sgRNA-A; B, *Met*-sgRNA-B; C, *Met*-sgRNA-C; D, *Met*-sgRNA-D; CD, *Met*-sgRNA-CD; ABCD, *Met*-sgRNA-ABCD.

target finder (http://targetfinder.flycrispr.neuro.brown.edu/). Forty-two potential off-target sites for 4 *Met* sgRNAs were identified. The alignment files of the sequences obtained using RNA isolated from *Met* knockout larvae were mapped to the *Ae. aegypti* reference genome; no insertions/deletions were detected in the RNA sequences at potential off-target sites. We also performed a variant analysis of the RNA sequences from WT and *Met* knockout larvae using samtools and bcftools (29, 30); the resulting alignment files were visualized by CLC genomics software. Again, no variants were detected at the potential off-target sites. Also, the black larval phenotype and mortality induced by *Met* knockout were not detected in any of the larvae developed from eggs injected with single or multiple sgRNAs targeting the *kmo* gene. The larvae that developed from eggs injected with single sgRNA or multiple sgRNAs targeting the *Met* gene showed black larval phenotype during only L3 and L4. The development of L1 and L2 stages appeared to be normal, and no abnormal phenotypes were detected in these larvae. Taken together, these data suggest that the black larval phenotype and mortality observed in larvae developed from the eggs injected with the sgRNA-targeting *Met* gene appear to be specific to knockout of the *Met* gene.

To further confirm the result that the black larval phenotype induced by knockout of the *Met* gene is due to a block in JH action, 3 sgRNAs targeting the *jhamt* (AAEL006280) gene were designed and synthesized (*SI Appendix*, Fig. S6*A*). When these 3 sgRNAs were injected into eggs to achieve a loss-of-function phenotype of the *jhamt* gene, only 3.2% of injected eggs hatched and the DNA isolated from larvae developed from injected eggs did not contain any mutations in the *jhamt* gene. Attempts at improving the hatch rate by application of JH III (10 μM) or methoprene (50 ng) were not successful. In *B. mori*, after knockout of the *jhamt* gene, without JH, the neonate larvae were unable to break the eggshell and hatch (14). The application of JH III or methoprene helped with hatching of some of the *jhamt* mutants. We also tested single sgRNA by injecting *jhamt*-sgRNA-B into 510 eggs from which 107 larvae hatched. During the L3 stage, 9% (10/107) of larvae showed black color body (*SI Appendix*, Fig. S6*B*) as seen in the larvae developed from eggs injected with *Met* sgRNAs. The larvae that showed the black larval phenotype died at the end of L4. Genomic DNA isolated from larvae that showed black color was used as a template to amplify the sgRNA target region of the *jhamt* gene, and the PCR products were sequenced. Mutations were detected in 4 of the 12 clones sequenced (*SI Appendix*, Fig. S6*C*).

To determine if *jhamt* expression is required for completion of embryonic development and/or hatching in *Ae. aegypti*, we compared embryonic development and hatch rate of uninjected eggs and those injected with *kmo* sgRNA-ABC, *jhamt* sgRNA-ABC, or *jhamt* sgRNA-B. Under our rearing conditions, segmentation of embryos is visible 24 h after egg laying (*SI Appendix*, Fig. S7). About 90% of embryos from uninjected or *kmo* sgRNA-ABC–injected eggs and 76% from *jhamt* sgRNA-B–injected eggs showed segmentation (*SI Appendix*, Figs. S8 and S9). The uninjected eggs or those injected with *kmo* sgRNA-ABC or *jhamt* sgRNA-B showed 91, 59, and 56% hatch rates, respectively (*SI Appendix*, Fig. S9). In contrast, only 20% of embryos from *jhamt* sgRNA-ABC–injected eggs showed segmentation, and 13% of them hatched (*SI Appendix*, Fig. S9). These data showed that the effect on embryonic development is more pronounced in *jhamt* multiple sgRNA-injected eggs when compared to those injected with *jhamt* single sgRNA. This might be due to higher levels of loss of function of the *jhamt* gene in multiple sgRNA-injected eggs when compared to that in eggs injected with single sgRNA. These data suggest that *Ae. aegypti* embryonic development may require *jhamt* gene expression. However, further research is required to understand the role of JH and identify its receptor during the embryonic development of *Ae. aegypti*.

Identification of Loss-of-Function Phenotypes by Coinjecting Single-Marker Gene sgRNA and Multiple-Target Gene sgRNAs. As described above, multiple sgRNAs induced *Met* gene knockout in G0. However, the *Met* gene knockout phenotypes were seen only in the L3 and L4 stages. It would be useful if the target gene knockout could be identified before the onset of the target gene phenotype because, in some cases, target genes may not show distinct phenotypes. To determine if it is possible to improve identification of target gene phenotypes by coinjecting the sgRNA targeting marker gene and the target gene, we tested multiple sgRNAs targeting *Met* and 1 sgRNA targeting *kmo*. A mixture of 1 *kmo* sgRNA (sgRNA-B) and 4 *Met* sgRNAs (sgRNA-A, sgRNA-B, sgRNA-C, and sgRNA-D) was injected into AAEL010097-Cas9 eggs. From 462 eggs injected, 243 larvae hatched. In the L2 stage, 40% (88/223) mosaic-eye larvae were identified. Interestingly, 75% (66/88) of the mosaic-eye larvae showed a black larval phenotype during the L3 and L4 stages (Fig. 1*D* and *SI Appendix*, Table S3). The mutations in the *kmo* and *Met* genes were confirmed by sequencing (*SI*

Appendix, Fig. S10). Two additional *kmo* and *Met* sgRNA injections were performed to confirm the results from the first experiment, and in these 2 experiments, 90 and 69% of mosaic-eye larvae showed a black larval phenotype (*SI Appendix*, Table S3). In 3 trials, injection of multiple *Met* sgRNAs and 1 *kmo* sgRNA showed that 78% of the marker gene mutants identified during L2 also showed the black larval phenotype during L3 and L4. In contrast, only 33% of the larvae exhibited the black larval phenotype in larvae hatched from eggs injected with only *Met* sgRNAs (Fig. 1*D*). These data demonstrate that injection of multiple sgRNAs targeting a marker gene and the gene of interest could significantly improve identification of mutants for the gene of interest in G0. Recent studies in *D. melanogaster* employed simultaneous targeting of a marker gene and a target gene (26) and a negative coselection strategy using a dominant female sterile allele (27) to improve screening efficiency for identification of CRISPR/Cas9-induced genome-editing events. These improvements could save labor and time involved in screening for mutants and facilitate identification of mutants of genes the knockout of which does not induce distinct phenotypes. The multiple sgRNA-based CRISPR/Cas9 genome-editing method reported in this paper adds another improvement to the genome-editing toolkit available for use in *Ae. aegypti* functional genomics studies.

Characterization of the Black Larval Phenotype Induced by *Met* Knockout. The black larval body color detected in *Met* mutants is similar to the black larval mutants discovered as natural variants in populations of *Manduca sexta* and other lepidopteran insects. In *M. sexta,* JH deficiency induces black melanized cuticle in the last larval instar, and application of JH during molting to the last larval instar prevents the appearance of the black larval phenotype (31). Similar phenotypes have been reported in other lepidopteran insects, including *Celerio euphorbiae*, *Papilio machaon*, and *Phalera bucephala* (32). Studies in *B. mori* and *D. melanogaster* showed that *ebony* and *yellow* genes are associated with larval color mutants (33, 34). In this study, JH analog methoprene was applied to rescue the L3 black larvae. Sixteen black larvae were maintained in 100 ng/μL methoprene and provided sufficient diet. None of the larvae were rescued and all of these larvae died later in the L4 stage. To determine mechanisms responsible for the black body color detected in *Met* knockout *Ae. aegypti* larvae, these mutants were further characterized using scanning (SEM) and transmission electron microscopy (TEM), RNA sequencing, and RT-qPCR. The WT L4 cuticle is lighter in color when compared to the pupal cuticle. Observation of *Met* knockout mutants under a stereomicroscope revealed 2 layers of cuticle, a transparent outer cuticle and a dark inner cuticle (Fig. 2*A*). Observations under the scanning electron microscope identified the outer layer of the cuticle as the larval cuticle similar to that seen in L4 larvae (Fig. 2*B*). The inner layer of cuticle in the *Met* mutant is similar to the pupal cuticle seen in 24-h-old pupae (Fig. 2*B*). To analyze the ultrastructure of abdominal cuticles from 24-h-old L4 WT and *Met* mutant larvae, TEM was performed. The cuticles of L4 WT larvae

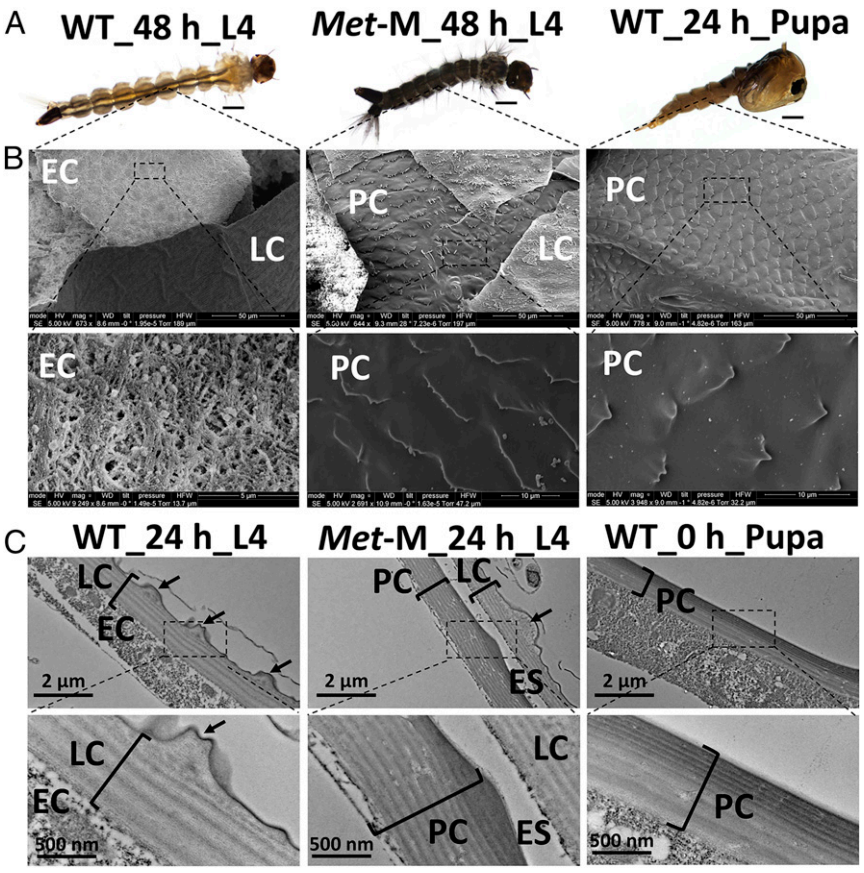

Fig. 2. *Met* mutants synthesize pupal cuticle during the larval stage. (*A*) Images of 48-h-old WT L4, 48-h-old *Met* knockout L4, and 24-h-old WT pupa are shown. (Scale bar, 1 mm.) (*B*) The SEM images of the cuticle from 48-h-old WT L4, 48-h-old *Met* knockout L4, and 24-h-old WT pupae. The staged larvae and pupae were fixed, critical-point-dried, coated, and photographed under a scanning electron microscope. To see the inner layer of WT and *Met* mutant cuticles, the outer layer of cuticle was peeled off using forceps. The *Bottom* panels show an enlarged view of marked areas. LC, larval cuticle; PC, pupal cuticle; EC, epidermal cell. (*C*) Ultrastructure of the larval body cuticle from WT and the *Met* mutant. Ultrastructure of the larval body cuticle from 24-h-old L4 WT, *Met* mutant, or WT pupa shortly after pupation was photographed under a transmission electron microscope. Arrows indicate the larval cuticle protuberances. (*Bottom*) An enlarged view of marked areas. LC, larval cuticle; EC, epidermal cell; ES, ecdysial space; and PC, pupal cuticle.

consist of a few less compact horizontal laminae and unique regular protuberances (arrows in Fig. 2*C*). However, there is no evidence of any pupal cuticle at this developmental stage (Fig. 2 *C*, *Left*). Unlike L4 WT larvae, there are 2 cuticles in the L4 *Met* mutant larvae (Fig. 2 *C*, *Middle*). The outer cuticle is similar to that of the WT L4 larval cuticle (Fig. 2 *C*, *Left*). In contrast, the inner cuticle is composed of a number of electron-dense compact horizontal laminae as seen in the pupal cuticle dissected from 0-h-old WT pupae (Fig. 2 *C*, *Right*). These data suggest that, unlike the WT strain, *Met* knockout larvae produced pupal cuticle precociously during the early stage of the last instar larvae.

Studies on variation in cuticle color in lepidopteran and other insects identified differential expression of genes coding for enzymes involved in melanization as one of the major contributors to the differences in cuticle color. To determine if any of the genes coding for enzymes involved in melanization are differentially expressed between WT and *Met* mutants, we sequenced RNA isolated from the AAEL010097-Cas9 strain (control) and black larval *Met* mutant larvae collected at 24 h after entering the L4 stage. Raw sequencing data statistics are presented in *SI Appendix*, Table S4. Differential gene expression between the WT and *Met* mutant was analyzed, and the overall gene expression differences are shown as the heatmap (Fig. 3*A*) and the volcano plot (Fig. 3*B*). Gene Ontology (GO) enrichment analysis was performed using the WEGO tool by plotting the GO information of the up- and down-regulated genes (*SI Appendix*, Figs. S11 and S12). Compared to WT, 417 genes were up-regulated, and 224 genes were down-regulated (≥2-fold, $P \leq 0.05$) in the *Met* knockout larvae. In *D. melanogaster*, the Wnt (35) and TGF-β (36) signaling pathways modulate JH action and synthesis, respectively. In the *Met* knockout larvae, genes involved in Wnt and the TGF-β signaling pathway were up-regulated (*SI Appendix*, Fig. S13*A*). Genes involved in other pathways such as the phagosome, AGE-RAGE signaling pathway in diabetic complication, neuroactive ligand-receptor interaction, mitophagy, apoptosis, glycine, serine and threonine metabolism, MAPK, and hippo are also up-regulated in the *Met* knockout larvae. Interestingly, most of the genes down-regulated in the *Met* knockout larvae seem to be involved in metabolic pathways, such as fatty acid metabolism (*SI Appendix*, Fig. S13*B*). Expression of the JH-response gene and transcription regulator *Kr-h1* (AAEL002390) was down-regulated (5.7-fold), but the expression of *Hairy* (AAEL005480, JH response gene, and transcription regulator), *BR-C* (AAEL008426), and *E93* (AAEL004572) was not significantly different between WT and *Met* mutants. This may be due to the depth and range of RNA-seq data and the variability among the biological replicates. The mRNA levels of these 4 genes were quantified by RT-qPCR. As shown in Fig. 3*C*, *Kr-h1* was down-regulated in L3 and L4 *Met* mutants, while *Hairy*, *BR-C*, and *E93* were down-regulated only in L4 *Met* mutants. In *Ae. aegypti*, the expression of *BR-C* and *E93* was lower during the pupal stage when compared to that in L4 (37). The *Met* mutant larvae proceeding to pupal stage seem to express lower levels of *BR-C* and *E93* when compared to the WT larvae.

The *Ae. aegypti* genome contains 10 genes coding for *prophenoloxidases* (*PPO*), while there are only 3 *PPO* genes in *D. melanogaster* (38). RNA-seq data showed up-regulation of 9 genes coding for enzymes, including PPO (PPO3 and PPO5), that are known to be involved in melanization. The RT-qPCR analysis showed that the *PPO3* gene was up-regulated in *Met* knockout L3, and the *PPO5* gene was up-regulated in *Met* knockout L4 larvae (Fig. 3*C*). The *dopa decarboxylase* (*DDC*) gene, which codes for another key in the melanization pathway was also up-regulated in *Met* knockout L3 larvae (Fig. 3*C*). The up-regulation of genes coding for enzymes involved in melanization in the *Met* mutant was confirmed by RT-qPCR (Fig. 3*D*). In *Ae. aegypti*, serine proteases and their inhibitors, serpins, carry out activation/inactivation of PPOs involved in melanization. Immune melanization proteases (IMP-1 and IMP-2) mediate PPO cleavage and immune response

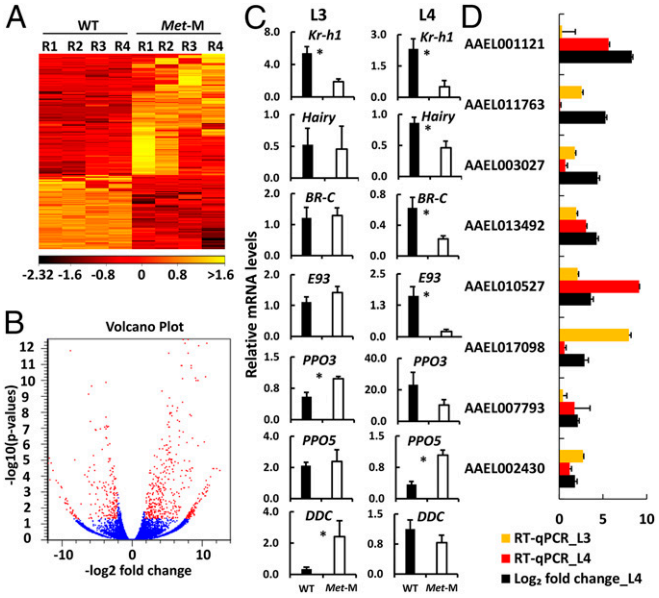

Fig. 3. Differential expression of genes in WT and *Met* mutant larvae. (*A*) The heat map displaying expression levels of mRNAs from L4 WT and the *Met* mutant. R1–R4 represent 4 biological replicates. (*B*) Volcano plot of differentially expressed genes in the WT and *Met* mutant larvae. The red dots indicate differentially expressed genes between WT and *Met* mutant larvae ($\log_2$ fold change ≥ 2, $P < 0.05$). (*C*) *Kr-h1*, *Hairy*, *BR-C*, *E93*, *DDC*, *PPO3*, and *PPO5* mRNA levels in L3 and L4 WT and the *Met* mutant determined by RT-qPCR. The data shown are mean + SE ($n = 3$). The asterisk indicates the significant differences between the 2 groups (*$P < 0.05$). *Met*-M, *Met* mutant. (*D*) Differential expression of genes coding for melanization enzymes in WT and *Met* mutants in L3 and L4 larvae determined by RNA-seq and RT-qPCR. The data shown are mean + SE (RNA-seq, $n = 4$; RT-qPCR, $n = 3$). The gene IDs are shown, and the names of these genes are listed in *SI Appendix*, Table S6.

against *Plasmodium* (38), and RNA sequencing identified 11 genes coding for serine proteases that are up-regulated in *Met* knockout larvae (Fig. 4*A*). Determining whether or not any of these proteases are involved in the activation of PPOs requires further studies. These data suggest that JH suppresses the expression of genes coding for enzymes involved in the melanization pathway in *Ae. aegypti*. In *Met* knockout larvae, the JH response is disabled, resulting in up-regulation of genes coding for enzymes including PPO and DDC involved in melanization. It appears that the black larval phenotype seen in *Met* knockout larvae is due to a combined effect on the expression of multiple genes coding for proteins involved in melanization. These data are in line with findings in other insects on the changes in the expression of multiple genes coding for proteins involved in the melanization pathway (39, 40).

RNA-seq data showed up-regulation of 54 genes coding for cuticle proteins in the *Met* knockout larvae. Blast2go annotation identified them to be coding for pupal or adult cuticle proteins, which included 11 adult cuticle proteins (Fig. 4*B* and *SI Appendix*, Table S5) (41). In adults, JH participates in the regulation of reproduction, including previtellogenic development, vitellogenesis, and oogenesis (15). *Early trypsin* is one of the first JH-regulated genes identified in *Ae. aegypti* (42). Female *Ae. aegypti* adults synthesize multiple trypsins after a blood meal, where the *early trypsin* is expressed in the midgut within 1 h after ingestion of a blood meal for 6 to 8 h. *Late trypsin* begins to express 8 to 10 h after the ingestion of a blood meal (42). RNA-seq data showed up-regulation of 16 trypsin and chymotrypsin genes, including JH-regulated *early* and *late trypsin* genes identified in *Ae. aegypti* adults in the *Met* knockout larvae (Fig. 4*C*). This suggests that the genes coding for digestive enzymes, that are normally expressed in the adults, are suppressed by JH during the larval stage. We also

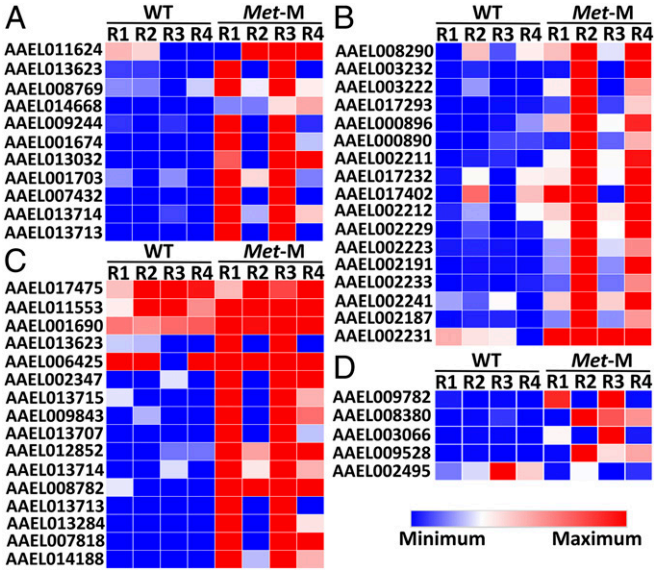

Fig. 4. Serine proteases (*A*), pupal and adult cuticle (*B*), trypsin and chymotrypsin (*C*), and chitinase (*D*) genes are up-regulated in L4 *Met* mutant larvae. The heatmaps of differentially expressed genes identified in RNA-seq data are shown. The heatmaps were prepared using Morpheus (https://software.broadinstitute.org/morpheus). The color code indicates the fold change in mRNA levels. The gene IDs are shown on the left side of the heatmap, and the names of pupal and adult cuticle genes are included in *SI Appendix*, Table S5. The names of serine proteases, trypsin, chymotrypsin, and chitinase genes are listed in *SI Appendix*, Table S7. R1–R4 represent 4 biological replicates.

found 4 chitinase genes that were up-regulated and 1 chitinase gene that was down-regulated in *Met* mutant larvae (Fig. 4*D*). These data suggest that JH suppresses the expression of pupal and adult genes during larval stages.

Interestingly, knockout of the *Met* gene did not affect the development of embryos and early larval instars. The black larval phenotype appeared during L3 and L4 stages of the mutant larvae that died before pupation. Studies on the developmental expression of *Ae. aegypti Met*, *jhamt*, and *Kr-h1* during larval stages detected these mRNAs throughout the larval stages (*SI Appendix*, Fig. S14). The *jhamt* mRNA levels showed 3 peaks during early L1, L2, and L3 stages, while *Met* and *Kr-h1* mRNA levels showed a single major peak at the beginning of L4 (*SI Appendix*, Fig. S14). Although the general requirement of JH to prevent precocious metamorphosis is similar to that reported in other insects, the black larval phenotype induced by *Met* knockout in *Ae. aegypti* appears to be unique. *Met* knockout in *B. mori* induced the development of pupal cuticle patches but not a complete black pupal cuticle (14). Induction of the black larval phenotype was also not reported in *D. melanogaster* larvae that had simultaneous *Met* mutation and *gce* deletion (7). The black larval phenotype was also not reported after RNA-mediated knockdown of *Met* in insects such as *T. castaneum* (4). Whether or not induction of the black larval phenotype is unique to *Ae. aegypti* remains to be investigated. The multiple sgRNA-based CRISPR/Cas9 method reported here could help to overcome some of the hurdles in gene knockout in *Ae. aegypti* and other insects. Future studies using these methods should help in making advances toward understanding the function of genes in *Ae. aegypti* and other insects.

Materials and Methods

Mosquito rearing, egg collection, microinjection, and mutagenesis analysis were performed using the methods described previously (17, 24). RNA isolation, RNA sequencing, and RT-qPCR were performed as described previously (43). Electron microscopy analysis was conducted as previously described (44). The details on the materials and methods used are included in *SI Appendix*.

ACKNOWLEDGMENTS. This work was supported by grants from the National Institutes of Health (GM070559-13) and the National Institute of Food and Agriculture, US Department of Agriculture (under HATCH Project 2351177000). We thank Jeff Howell for help with insect rearing and reading the earlier version of the manuscript and Robert A. Harrell II, Channa Aluvihare, and Omar S. Akbari for help with embryonic injections, *Ae. aegypti* rearing, and the AAEL010097-Cas9 strain.

1. L. M. Riddiford, Cellular and molecular actions of juvenile hormone I. General considerations and premetamorphic actions. *Adv. Insect Physiol.* **24**, 213–274 (1994).
2. M. Jindra, S. R. Palli, L. M. Riddiford, The juvenile hormone signaling pathway in insect development. *Annu. Rev. Entomol.* **58**, 181–204 (2013).
3. T. G. Wilson, J. Fabian, A *Drosophila melanogaster* mutant resistant to a chemical analog of juvenile hormone. *Dev. Biol.* **118**, 190–201 (1986).
4. B. Konopova, M. Jindra, Juvenile hormone resistance gene Methoprene-tolerant controls entry into metamorphosis in the beetle *Tribolium castaneum*. *Proc. Natl. Acad. Sci. U.S.A.* **104**, 10488–10493 (2007).
5. M. A. Abdou *et al.*, *Drosophila* Met and Gce are partially redundant in transducing juvenile hormone action. *Insect Biochem. Mol. Biol.* **41**, 938–945 (2011).
6. J. P. Charles *et al.*, Ligand-binding properties of a juvenile hormone receptor, Methoprene-tolerant. *Proc. Natl. Acad. Sci. U.S.A.* **108**, 21128–21133 (2011).
7. M. Jindra, M. Uhlirova, J. P. Charles, V. Smykal, R. J. Hill, Genetic evidence for function of the bHLH-PAS protein Gce/Met as a juvenile hormone receptor. *PLoS Genet.* **11**, e1005394 (2015).
8. M. Li *et al.*, A steroid receptor coactivator acts as the DNA-binding partner of the methoprene-tolerant protein in regulating juvenile hormone response genes. *Mol. Cell. Endocrinol.* **394**, 47–58 (2014).
9. Z. Zhang, J. Xu, Z. Sheng, Y. Sui, S. R. Palli, Steroid receptor co-activator is required for juvenile hormone signal transduction through a bHLH-PAS transcription factor, methoprene tolerant. *J. Biol. Chem.* **286**, 8437–8447 (2011).
10. T. Kayukawa *et al.*, Krüppel Homolog 1 inhibits insect metamorphosis via direct transcriptional repression of *Broad-Complex*, a pupal specifier gene. *J. Biol. Chem.* **291**, 1751–1762 (2016).
11. T. Kayukawa, A. Jouraku, Y. Ito, T. Shinoda, Molecular mechanism underlying juvenile hormone-mediated repression of precocious larval-adult metamorphosis. *Proc. Natl. Acad. Sci. U.S.A.* **114**, 1057–1062 (2017).
12. A. Tan, H. Tanaka, T. Tamura, T. Shiotsuki, Precocious metamorphosis in transgenic silkworms overexpressing juvenile hormone esterase. *Proc. Natl. Acad. Sci. U.S.A.* **102**, 11751–11756 (2005).
13. T. Daimon *et al.*, Precocious metamorphosis in the juvenile hormone-deficient mutant of the silkworm, *Bombyx mori*. *PLoS Genet.* **8**, e1002486 (2012).
14. T. Daimon, M. Uchibori, H. Nakao, H. Sezutsu, T. Shinoda, Knockout silkworms reveal a dispensable role for juvenile hormones in holometabolous life cycle. *Proc. Natl. Acad. Sci. U.S.A.* **112**, E4226–E4235 (2015).
15. S. Roy, T. T. Saha, Z. Zou, A. S. Raikhel, Regulatory pathways controlling female insect reproduction. *Annu. Rev. Entomol.* **63**, 489–511 (2018).
16. S. W. Shin, Z. Zou, T. T. Saha, A. S. Raikhel, bHLH-PAS heterodimer of methoprene-tolerant and Cycle mediates circadian expression of juvenile hormone-induced mosquito genes. *Proc. Natl. Acad. Sci. U.S.A.* **109**, 16576–16581 (2012).
17. S. Basu *et al.*, Silencing of end-joining repair for efficient site-specific gene insertion after TALEN/CRISPR mutagenesis in *Aedes aegypti*. *Proc. Natl. Acad. Sci. U.S.A.* **112**, 4038–4043 (2015).
18. S. Dong *et al.*, Heritable CRISPR/Cas9-mediated genome editing in the yellow fever mosquito, *Aedes aegypti*. *PLoS One* **10**, e0122353 (2015).
19. A. B. Hall *et al.*, Sex determination. A male-determining factor in the mosquito *Aedes aegypti*. *Science* **348**, 1268–1270 (2015).
20. M. Li *et al.*, Germline Cas9 expression yields highly efficient genome engineering in a major worldwide disease vector, *Aedes aegypti*. *Proc. Natl. Acad. Sci. U.S.A.* **114**, E10540–E10549 (2017).
21. L. Ling, V. A. Kokoza, C. Zhang, E. Aksoy, A. S. Raikhel, MicroRNA-277 targets *insulin-like peptides 7* and *8* to control lipid metabolism and reproduction in *Aedes aegypti* mosquitoes. *Proc. Natl. Acad. Sci. U.S.A.* **114**, E8017–E8024 (2017).
22. L. Ling, A. S. Raikhel, Serotonin signaling regulates insulin-like peptides for growth, reproduction, and metabolism in the disease vector *Aedes aegypti*. *Proc. Natl. Acad. Sci. U.S.A.* **115**, E9822–E9831 (2018).
23. Y. Zhang *et al.*, microRNA-309 targets the Homeobox gene *SIX4* and controls ovarian development in the mosquito *Aedes aegypti*. *Proc. Natl. Acad. Sci. U.S.A.* **113**, E4828–E4836 (2016).
24. K. E. Kistler, L. B. Vosshall, B. J. Matthews, Genome engineering with CRISPR-Cas9 in the mosquito *Aedes aegypti*. *Cell Rep.* **11**, 51–60 (2015).
25. D. T. Ge, C. Tipping, M. H. Brodsky, P. D. Zamore, Rapid screening for CRISPR-directed editing of the *Drosophila* genome using white coconversion. *G3 (Bethesda)* **6**, 3197–3206 (2016).
26. N. S. Kane, M. Vora, K. J. Varre, R. W. Padgett, Efficient screening of CRISPR/Cas9-induced events in *Drosophila* using a co-CRISPR strategy. *G3 (Bethesda)* **7**, 87–93 (2017).
27. B. Ewen-Campen, N. Perrimon, *ovo*^{D} co-selection: A method for enriching CRISPR/Cas9-edited alleles in *Drosophila*. *G3 (Bethesda)* **8**, 2749–2756 (2018).

28. S. J. Gratz *et al*., Highly specific and efficient CRISPR/Cas9-catalyzed homology-directed repair in *Drosophila*. *Genetics* **196**, 961–971 (2014).
29. H. Li *et al*., The sequence alignment/map format and SAMtools. *Bioinformatics* **25**, 2078–2079 (2009).
30. V. Narasimhan *et al*., BCFtools/RoH: A hidden Markov model approach for detecting autozygosity from next-generation sequencing data. *Bioinformatics* **32**, 1749–1751 (2016).
31. L. Safranek, L. Riddiford, The biology of the black larval mutant of the tobacco hornworm, *Manduca sexta*. *J. Insect Physiol.* **21**, 1931–1938 (1975).
32. I. Kayser-Wegmann, Differences in black pigmentation in lepidopteran cuticles as revealed by light and electron microscopy. *Cell Tissue Res.* **171**, 513–521 (1976).
33. R. Futahashi *et al*., *yellow* and *ebony* are the responsible genes for the larval color mutants of the silkworm *Bombyx mori*. *Genetics* **180**, 1995–2005 (2008).
34. J. E. Pool, C. F. Aquadro, The genetic basis of adaptive pigmentation variation in *Drosophila melanogaster*. *Mol. Ecol.* **16**, 2844–2851 (2007).
35. M. Abdou *et al*., Wnt signaling cross-talks with JH signaling by suppressing *Met* and *gce* expression. *PLoS One* **6**, e26772 (2011).
36. J. Huang *et al*., DPP-mediated TGFbeta signaling regulates juvenile hormone biosynthesis by activating the expression of juvenile hormone acid methyltransferase. *Development* **138**, 2283–2291 (2011).
37. Y. Wu, R. Parthasarathy, H. Bai, S. R. Palli, Mechanisms of midgut remodeling: Juvenile hormone analog methoprene blocks midgut metamorphosis by modulating ecdysone action. *Mech. Dev.* **123**, 530–547 (2006).
38. Z. Zou, S. W. Shin, K. S. Alvarez, V. Kokoza, A. S. Raikhel, Distinct melanization pathways in the mosquito *Aedes aegypti*. *Immunity* **32**, 41–53 (2010).
39. K. Hiruma, L. M. Riddiford, The molecular mechanisms of cuticular melanization: The ecdysone cascade leading to dopa decarboxylase expression in *Manduca sexta*. *Insect Biochem. Mol. Biol.* **39**, 245–253 (2009).
40. J. R. True, Insect melanism: The molecules matter. *Trends Ecol. Evol.* **18**, 640–647 (2003).
41. J. Zhu, J. M. Busche, X. Zhang, Identification of juvenile hormone target genes in the adult female mosquitoes. *Insect Biochem. Mol. Biol.* **40**, 23–29 (2010).
42. F. G. Noriega, M. A. Wells, A molecular view of trypsin synthesis in the midgut of *Aedes aegypti*. *J. Insect Physiol.* **45**, 613–620 (1999).
43. A. Roy, S. R. Palli, Epigenetic modifications acetylation and deacetylation play important roles in juvenile hormone action. *BMC Genomics* **19**, 934 (2018).
44. M. Y. Noh *et al*., Two major cuticular proteins are required for assembly of horizontal laminae and vertical pore canals in rigid cuticle of *Tribolium castaneum*. *Insect Biochem. Mol. Biol.* **53**, 22–29 (2014).